



**AIAA 98-2697**

**Wake Imaging in Supersonic Facilities  
Using the Iodine Cordes Bands**

R.J. Exton, R. Jeffrey Balla  
B. Shirinzadeh, M.E. Hillard,  
and Gregory J. Brauckmann  
NASA Langley Research Center  
Hampton, VA 23681-2199

**20th AIAA Advanced Measurement  
and Ground Testing Technology  
Conference**

**June 15-18, 1998 / Albuquerque, NM**

## WAKE IMAGING IN SUPERSONIC FACILITIES USING THE IODINE CORDES BANDS

R. J. Exton,\* R. Jeffrey Balla,\* B. Shirinzadeh,\*  
 M. E. Hillard,\* and Gregory J. Brauckmann†  
 NASA Langley Research Center  
 Hampton, VA 23681-2199

ABSTRACT

We demonstrate a new method for visualizing the near-wake region of aerodynamic models in supersonic air flows. Experiments were performed in the 15-inch Mach 6 High-Temperature Tunnel at NASA Langley Research Center. We performed "local" flow seeding using less than 0.01 grams of iodine per wind tunnel run. We painted a small area  $1 \times 4$  cm on the front of a ceramic 38.1 mm diameter cylindrical model using tincture of iodine. When injected into the supersonic flow, the model surface is heated. The iodine vaporizes, entrains into the boundary layer, follows the model contour, enters the shear layer, and eventually mixes into the wake region. Planar laser-induced fluorescence (PLIF) was generated by exciting the Iodine Cordes Bands using a narrowband pulsed ArF excimer laser. Instantaneous images 20 mm wide were obtained by detecting approximately  $3 \times 10^{12}$  molecules/cm<sup>3</sup> iodine in approximately  $1.8 \times 10^{17}$  molecules/cm<sup>3</sup> air using a CCD camera. This is the first application of "local" seeding using iodine excitation in the Cordes bands for optical diagnostics.

---

\*Optical Physicist, Measurement Science and Technology Branch, Fluid Mechanics and Acoustics Division, Research and Technology Group

†Aerospace Engineer, Aerothermodynamics Branch, Aero and Gas Dynamics Division, Research and Technology Group, Senior Member AIAA.

Copyright © 1998 by the American Institute of Aeronautics and Astronautics, Inc. No copyright is asserted in the United States under Title 17, U.S. Code. The U.S. Government has a royalty-free license to exercise all rights under the copyright claimed herein for Governmental purposes. All other rights are reserved by the copyright owner.

INTRODUCTION

This paper presents preliminary results in the development of a new non-intrusive optical diagnostic method for studying the near-wake region created by bodies in flows at supersonic and hypersonic speeds. Horvath<sup>8</sup> has summarized the importance of near-wake measurements and visualization in high-speed flows to understand a variety of aerodynamic problems. These include aerobraking, planetary probes with payloads, fuel-air mixing in scramjet combustors, and anti-armor projectiles in flight. Data is required on the unsteadiness, mixing, separation and reattachment points, and shear layer characteristics such as temperature, density and transition location. Data are also useful for computational fluid dynamic (CFD) code validation, especially in turbulent flows. We take the first step toward new quantitative wake diagnostics. We demonstrate near-wake visualization using PLIF created by exciting iodine in the Cordes Bands using an ArF excimer laser near 193 nm.

In many wake studies, data are obtained using traditional techniques including Schlieren photography, pitot tubes, and hot-wire anemometry. Practical problems, typical instrumentation, and a brief review of the literature and characteristics of the near wakes generated by supersonic flows are discussed in an experimental study at Mach 6 by Horvath<sup>8</sup>. The low densities (typically  $0.3\text{--}30 \times 10^{16}$  molecules/cm<sup>3</sup>) encountered limit the usefulness of many techniques. Results demonstrate the need for new diagnostic methods.

Several optical diagnostic methods are applicable. Many are discussed in a book edited by Boutier<sup>2</sup>. Muntz<sup>17</sup> used electron beam fluorescence to measure density. They discuss the problems involved in extending this technique above its traditional limit of

$1 \times 10^{15}$  molecules/cm<sup>3</sup>. Merzkirch<sup>13</sup> surveys schlieren photography and shadowgraphy, which provide two dimensional cross-sectional flow information. Focused schlieren techniques have been developed by Gartenberg<sup>5</sup> to enhance the line-of-sight resolution. Shirinzadeh<sup>20</sup> demonstrated quantitative Rayleigh scattering in the near-wake under Mach 6 freestream conditions. Planar imaging of  $1.8 \times 10^{17}$  molecules/cm<sup>3</sup> air was possible by averaging 45 laser shots. This laser-based method provides high spatial (~1 mm) and temporal (~15 ns) resolution.

LIF-based optical diagnostic methods are useful in low density wake flows since they can produce large signals using trace amounts of a species. Often, these species can be seeded. For example, Miles<sup>15</sup> seeded sodium to view the flow of hypersonic helium. McDaniel<sup>12</sup> seeded iodine for quantitative (off-resonant) measurements using visible fluorescence. Kychakoff<sup>9</sup> monitored fluorescence from combustion gases seeded with NO.

LIF-based iodine diagnostics have an extensive history as a molecular seed for high density flows. Many iodine properties, and contributions from many authors including McDaniel<sup>12</sup>, Hansen<sup>7</sup>, and others has been reviewed by Hiller<sup>7</sup>. Visualization and measurements of pressure, temperature, density, and velocity have been obtained. In many cases results are obtained by exciting P13/R15 transitions from  $B^3 \pi_{ou}^+$  ( $v'=43$ )  $\leftarrow X^1 \Sigma_g^+$  ( $v''=0$ ) with an Ar<sup>+</sup> laser at 514.5 nm. Visible excitation characteristics are: absorption cross section =  $2.2 \times 10^{-18}$  cm<sup>2</sup> (Tellinghuisen, 1982), visible fluorescence quantum efficiency < 0.5 (Brewer and Tellinghuisen, 1972), and natural lifetime = 2  $\mu$ s (Hiller and Hansen, 1990). This method requires large quantities of seeded iodine. For large-scale facilities this method produces unacceptable facility corrosion and health risks.

The present iodine method differs from previous studies by using an ArF excimer laser operating at 193 nm to excite the iodine Cordes bands ( $D^1 \Sigma_u^+ \leftarrow X^1 \Sigma_g^+$ ). Resulting transitions are of the charge-transfer type between ion-pair excited states and valence ground states. These strongly allowed transitions have many favorable attributes including a large cross section ( $1 \times 10^{-17}$  cm<sup>2</sup>) (Myer and Samson, 1970), fluorescence quantum yield near 1 (McCusker et al. 1975 and Shaw et al. 1980), and short fluorescence lifetime of 15.5 ns (Callear et al., 1976). LIF signals are larger, and smaller quantities of seed are required.

We present initial results of flow-visualization experiments in the near-wake region generated by a

simple model in a Mach 6 flow. The goal is to demonstrate that trace amounts of “locally” seeded iodine excited by an ArF excimer laser at 193 nm are sufficient for visualization under these low-density conditions. “Local” seeding refers to the introduction of trace amounts of iodine, which are adsorbed in a thin surface layer of a model. This creates a model with a built-in but finite source of iodine. When injected into the supersonic flow, the model surface is heated. The iodine vaporizes, entrains into the boundary layer, follows the model contour, enters the shear layer, and eventually mixes into the wake region. The near-wake is illuminated by a thin laser sheet. The resulting iodine PLIF is viewed at 90 degrees by a charge-coupled-device (CCD) camera. This produces instantaneous planar LIF snapshots of the near-wake flow.

## EXPERIMENTAL

Experiments were performed in a Mach 6 facility using ceramic models. The apparatus and configuration are similar to those employed by Shirinzadeh<sup>20</sup>. We present only a brief description here. A simplified schematic drawing of the experimental arrangement is shown in Figure 1. We performed “local” flow seeding using trace quantities of iodine. We paint a small area on the front of a cylindrical model using tincture of iodine. The iodine is detected in the near-wake using a pulsed narrowband ArF excimer laser. The laser beam is focused using cylindrical lenses into a sheet. The beam enters the facility from above through a suprasil quartz window and is dumped at the bottom of the test section. A CCD camera views the laser sheet at 90 degrees through a recessed suprasil quartz window. Once positioned, the laser beam and camera remain fixed for a given test sequence. Different regions of the wake are viewed by translating the model in the flow direction.

### Mach 6 Facility

Tests were performed in the NASA Langley 15-inch Mach 6 High-Temperature Tunnel. Micol<sup>4</sup> presents a detailed facility description which is summarized here. It is a conventional blowdown-to-vacuum wind tunnel that uses dry air as the test gas. The air is electrically heated prior to expansion through the Mach 6 nozzle. The test section is an open jet type with a test cabin that is approximately 1.8 m long and an internal diameter of 1.5 m. The flow from the Mach 6 axisymmetric, contoured nozzle exhausts into the test cabin, traverses the model test region, and is collected by the diffuser. Models can be injected into the flow in 1 to 2 sec. Typical test runs last from 30 to 60 sec. The facility

operates with stagnation pressures from 0.31 to 2.48 Mpa (45–360 psia) and stagnation temperatures up to 700K (800°F). The unit Reynolds number ranges from  $1.6$  to  $19.7 \times 10^6 \text{ m}^{-1}$ . Typical run conditions for the models tested here are 2.07 MPa (300 psia) and 589K (600°F). Free-stream velocity is 1020 m/sec.

#### Excimer laser

The ArF excimer laser is operated in a narrowband mode at 193 nm. It is mounted above the test section. The laser is tuned between the rotational transitions of the (4,0) vibrational band of the oxygen Schumann-Runge system near the peak of the laser gain profile. This setting minimizes laser-beam absorption through room air. The laser bandwidth is approximately  $1 \text{ cm}^{-1}$ . In this case, the iodine absorption spectrum is nearly a continuum. The laser operates at a pulse repetition rate of 10 Hz. Each pulse generates approximately 100 mJ with a pulse duration of 15 nsec. The laser beam is shaped by cylindrical lenses and apertures. It is directed down into the test section through a suprasil window. In the wake, this ribbon beam is approximately 0.5 mm thick and 20 mm wide and contains about 50 mJ/pulse. The short pulse duration effectively “freezes” the motion of the flow.

#### CCD Camera

Emission is collected using a Cassegrain lens with a 90 mm focal length (f/1.1). A Schott BG-24 filter rejects scattered laser light at 193 nm and transmits the fluorescence from 210 to 600 nm. Emission is detected using a gated, single-stage intensified, interline transfer CCD camera. It consists of a two dimensional pixel array (768 horizontal by 494 vertical) with dimensions  $7.8 \mu\text{m}$  by  $9.1 \mu\text{m}$  respectively. It uses an S-20Q photocathode with response from 185 to 600 nm. Photocathode quantum efficiency is 20% at 210 nm and 24% at 340 nm. The camera views the flow through a side window that is recessed into the test section for better light gathering. The effective resolution is approximately 1 mm in the plane of the laser ribbon. We use an intensifier gate width of 400 nsec to reject extraneous light. Data is acquired at 10 Hz using a framegrabber with 8-bit digitizer and stored in a computer for subsequent analysis. Forty five images filled available memory. The video signal was sent to a video cassette recorder to record the entire tunnel run.

#### Models and seeding

Most models designed for these proof-of-concept tests are constructed of ceramic (fused silica). Phosphor coated ceramic models are routinely employed at NASA Langley Research Center for global surface temperature measurements. A simple seeding technique is used. We paint a small area of the ceramic 38.1 mm diameter cylindrical model at the stagnation point with a tincture of iodine. The tincture consists of 1 gm of crystalline iodine that is dissolved in 12.5 ml of ethanol (a saturated solution). For each test run, several drops of this solution are painted on the surface. This solution typically covers an area of  $1 \times 4 \text{ cm}$ . This ensures overlap of the seeded flow with the laser beam. The ethanol evaporates during facility pumpdown prior to each run. This leaves iodine in a thin ( $\sim 0.5 \text{ mm}$ ) surface layer of the ceramic model.

### RESULTS AND DISCUSSION

#### Iodine Spectroscopy

Iodine Cordes Band excitation and the resulting emission occur by a complex mechanism. Many rotational, vibrational and electronic states are involved. Some details of the spectroscopy are not understood. We present a simplified description of the spectroscopy to explain these flow visualization results. Potential energy curves for the Cordes Band ( $D^1\Sigma_u^+ \leftarrow X^1\Sigma_g^+$ ) excitation process and major D state removal processes are shown in Figure 2. Minor processes are ignored; details can be found in Hemmati<sup>6</sup> and Martin<sup>10</sup>.

Molecular iodine exhibits absorption in the Cordes bands from 175 to 200 nm, as reported by Myer and Samson<sup>18</sup>. This broad absorption band is conveniently excited using the ArF excimer laser at 193 nm. Figure 3 shows the fluorescence emission spectrum from 188 to 340 nm obtained in our lab by exciting  $7.2 \times 10^{15} \text{ molecules/cm}^3$  (0.22 Torr) pure iodine at 193 nm in a 1 cm square cell at 295K.

Emission from 188–250 nm is due to discrete (bound-bound) transitions (Venkateswarlu, 1970). Emission in the 250 to 500 nm region is due to the McLennan bands. Emission is composed of diffuse regions and a highly structured (bound-free) continuum near 325 nm. The McLennan bands represent one of the few examples in molecular spectroscopy of Condon's internal diffraction effect (Tellinghuisen, 1974; 1984).

The fluorescence emission spectrum is recorded with an optical multichannel analyzer (OMA) with a S-20 detector response. Spectral response of the system is calibrated with a deuterium lamp in place of the cell, which results in a significant correction (approximately a factor of 40) to the strength of the discrete spectrum relative to the McLennan bands. Neither the discrete spectrum nor the McLennan bands are resolved here.

Increasing pressure alters the emission spectrum. Collisions with buffer gas molecules transfer the population from the  $D^1\Sigma_u^+$  state that is responsible for the bound-bound emission and McLennan bands to the  $D'^3\Pi_{2g}$  state. Emission from the latter ( $D'^3\Pi_{2g} \rightarrow A'\pi_{2u}$ ) produces the 340 nm band (Mulliken, 1971 and Tellinghuisen, 1977). Several weaker visible bands are produced from other collisionally-populated excited states (Martin et al. 1981). Under the conditions present in this near-wake flow, signals from these transitions are negligible.

#### Aerodynamic Test Results

Several simple aerodynamic models were constructed to demonstrate this visualization method. Figure 4 shows a composite view of the wake of a truncated cylinder model at Mach 6. The model is positioned during sequential runs so that the laser ribbon intercepts three overlapping positions (A, B, and C) in the model wake. The leading edge of the laser beam at position A is located approximately 25 mm from the center of the model. The three images (A, B, and C) are cropped according to their positions as measured prior to each run and superimposed to illustrate the overall character of the wake. Due to temperature sensitive movement of the model support from run to run, the position of the laser sheets relative to the model are only known to  $\pm 2$  mm.

When the model is injected into the flow, the iodine fluorescence is bright and erratic. Thus, we wait for approximately 10 sec, during which the iodine fluorescence decreases by more than an order of magnitude and stabilizes. Then, data are acquired for approximately 10 to 20 sec. Seeding at the stagnation point enhances both the upper and lower shear layers, as can be seen at position A. Individual frames show that unsteadiness in the flow increases significantly from position A to C. Images at positions A and B are shown as averages of 44 frames. In contrast, a single frame is shown for position C. In this region, the flow becomes unsteady and individual frames differ significantly.

In earlier work, Shirinzadeh<sup>20</sup> performed quantitative planar Rayleigh scattering measurements in this facility. Models, facility conditions, instrumentation, and optical geometries were identical to those used in this iodine study. This allows comparison between the flow fields and signal levels observed with both techniques. Rayleigh results indicate near-wake air densities are approximately  $1.8 \times 10^{17}$  molecules/cm<sup>3</sup>. Iodine PLIF signals in the near-wake region were approximately 60 times greater than the Rayleigh signal. Subsequent lab measurements, taken with a quartz cell in the same geometry, indicate that the density of iodine in the near-wake is approximately  $3 \times 10^{12}$  molecules/cm<sup>3</sup>.

Iodine optical saturation was studied following the tunnel experiments. Fluorescence measurements were taken using an optical multichannel analyzer while attenuating the excitation beam at 193 nm with calibrated neutral density filters. These results, shown in Figure 5, illustrate the onset of optical saturation in the bound-bound transitions measured using fluorescence from the strongest peak of the McLennan band at 325 nm with  $3 \times 10^{16}$  molecules/cm<sup>3</sup> (1 torr) air as the buffer gas. The fluorescence signal varies linearly with laser power density to approximately 0.1 MW/cm<sup>2</sup>. The Mach 6 tunnel measurements were conducted at approximately 30 MW/cm<sup>2</sup>. Hence, all images including Figure 4 were acquired using iodine transitions that were optically saturated. Hence, a wider laser sheet could be used to capture regions A, B, and C in Figure 4 simultaneously with minimal loss of signal.

Seeding at several model locations was tested to enhance specific regions of the flow. Cylindrical ceramic model wakes were observed in which the seeding was applied at 90°, 180°, and 270° (measured clockwise from the stagnation point located at 0°). Fluorescence from the near-wake between the shear layers in region A was uniform for each case. Seeding at 90° or 270° only enhanced the upper or lower shear layers, respectively. Neither shear layer is enhanced when seeding is applied in the wake region (180°).

An aluminum cylindrical model was also tested. A slot (1 × 1 × 5 mm) was milled into the model at the stagnation point. A piece of porous ceramic was cemented into the slot. Iodine seeding using the ceramic insert produced images similar to Figure 4. This demonstrates a simple method for seeding in flows surrounding non-ceramic models.

This "local" seeding technique is simple and easy to implement. It offers the following advantages: (1) the

location of the seed source can be chosen judiciously to emphasize selectable regions of the flow, (2) laser-beam absorption and fluorescence trapping are minimized, and (3) trace amounts of iodine limits concerns about toxicity, facility corrosion, and the requirement for specially designed facilities (Hiller and Hansen, 1990) normally encountered with the use of this molecule. This method adds less than 0.01 gm of iodine to the facility per run. In addition, the large Cordes Band absorption cross section generates strong fluorescence for trace amounts of iodine. This reduces seeding-related perturbations on the observed flow.

This technique offers the potential for global visualization of near-surface flow features. In our lab, we formed the laser into a  $25 \times 25$  mm beam and directly illuminated a model surface. Using appropriate filters, fast gating of the CCD camera, and judiciously selecting the model material, we have demonstrated that unwanted scattered laser light and model fluorescence can be rejected. The CCD camera sees fluorescence mainly from iodine entrained in the flow. This suggests that in a model flow field boundary layer features such as turbulent spots, streaks, and vortices may become visible. This may allow visualization of near-body flow streamlines and global visualization of the transition from laminar to turbulent flow. In the opinion of Bogdanov, the most critical test in CFD validation would be "the experimental determination of specific streamlines in complex three-dimensional flows, and a comparison of these streamline paths to computation." The ArF laser-based excitation of locally seeded iodine may provide the experimental method for this validation. Future wind tunnel entries are planned to test this idea. We are also investigating the potential of this method for new quantitative wake diagnostics.

### CONCLUSIONS

We demonstrate a new method for visualizing the near-wake region of models in supersonic air flows. We combine "local" seeding of trace quantities of iodine with planar laser-induced fluorescence generated by exciting the iodine Cordes bands using an ArF excimer laser. Instantaneous near-wake images 20 mm wide were obtained by detecting approximately  $3 \times 10^{12}$  molecules/cm<sup>3</sup> of iodine in approximately  $1.8 \times 10^{17}$  molecules/cm<sup>3</sup> of air using a single-intensified CCD camera. To our knowledge, this is the first application of "local" seeding using iodine excitation in the Cordes bands for optical diagnostics.

With continued development, the authors expect this technique will have many applications.

### ACKNOWLEDGMENTS

The authors thank Charles G. Miller, III for providing facility time and aerodynamic discussions for these experiments. The authors also acknowledge helpful discussions with G.C. Herring and electronic and mechanical design contributions from R.W. Gregory, B.W. Barnes, and W.E. Lipford.

### REFERENCES

1. Bogdanov, S.M., Comments on experiments for computational validation for fluid dynamic predictions. In: Hypersonic flows for reentry problems. (eds. Desideri J.A., R. Glowinski, J. Periaux). Vol. 1, pp. 12-17, Berlin, Springer-Verlag, 1991.
2. Boutier, A., editor., New Trends in Instrumentation for Hypersonic Research, Kluwer Academic Publishers, 1993.
3. Brewer, L. and J. Tellinghuisen, Quantum yield for unimolecular dissociation of I<sub>2</sub> in visible absorption, *J. Chem. Phys.* 56, pp. 3929-3938 (1972).
4. Callear, A.B., P. Erman, and J. Kurepa, The D state lifetime and the UV laser action of molecular iodine, *Chem. Phys. Lett.* 44, pp. 599-601 (1976).
5. Gartenberg, E., L.M. Weinstein, E.E. Lee, Aerodynamic investigation with focusing schlieren in a cryogenic wind tunnel. *AIAA Journal*, Vol. 32, pp. 1242-1249 (1994).
6. Hemmati, H., and G.J. Collins, Laser excited fluorescence of I<sub>2</sub>, *Chem. Phys. Lett.* 75, pp. 488-493 (1980).
7. Hiller, B., and R.K. Hanson, Properties of the iodine molecule relevant to laser-induced fluorescence experiments in gas flows. *Exp. Fluids* 10, pp. 1-11 (1990).
8. Horvath, T.J., C.B. McGinley, K. Hannemann, "Blunt body near wake flow field at Mach 6," AIAA-96-1935, 27th AIAA fluid dynamics conference, New Orleans, LA, June 1996.

9. Kychakoff G., K. Knapp, R.D. Howe, and R.K. Hanson, Flow visualization in combustion gases using nitric oxide fluorescence. *AIAA Journal* Vol. 22, pp. 153–154 (1984).
10. Martin, M., C. Fotakis, R.J. Donovan, and M.J. Shaw, Optical pumping and collisional quenching of  $I_2$  ( $D^1\Sigma_u^+$ ) IL Nuovo Cimento B 63, pp. 300–308 (1981).
11. McCusker, M.V., R.M. Hill, D.L. Heustis, D.C. Lorents, R.A. Gutchev, and H.H. Nakano, The possibility of an efficient tunable molecular iodine laser near 340 nm., *Appl. Phys. Lett.* 27, pp. 363–365 (1975).
12. McDaniel, J.C., D. Baganoff, and R.L. Byer, Density measurement in compressible flows using off-resonant laser-induced fluorescence. *Phys. Fluids*. 25, pp. 1105–1107 (1982).
13. Merzkirch W., Flow visualization. 2nd ed. London, Academic Press (1987).
14. Micol, J.R., Hypersonic aerodynamic/aerothermodynamic testing capabilities at Langley research center: aerothermodynamic facilities complex, AIAA-95-2107, 30th AIAA Thermophysics conference, San Diego, CA, June 1995.
15. Miles R.B., E. Udd, and M. Zimmerman, Quantitative flow visualization in sodium vapor seeded hypersonic helium. *Appl. Phys. Lett.* 32, pp. 317–319 (1978).
16. Mulliken, R.S., Iodine Revisited, *J. Chem. Phys.* 55, pp. 288–309 (1971).
17. Muntz, E.P., and D.A. Erwin, Rapid pulse electron beam fluorescence for flow field diagnostics, In: New Trends in Instrumentation for Hypersonic Research. (Boutier, A., editor). pp. 265–273, Kluwer Academic Publishers, 1993.
18. Myer, J.A., and J.A.R. Samson, Absorption cross section and photo ionization yield of  $I_2$  between 1050 and 2200 Å., *J. Chem. Phys.* 52, 716–718 (1970).
19. Shaw, M.J., C.B. Edwards, F. O'Neill, C. Fotakis, and R.J. Donovan, Efficient laser action on the 342-nm band of molecular iodine using ArF laser pumping, *Appl. Phys. Lett.* 37, 346–348 (1980).
20. Shirinzadeh, B., R.J. Balla, and M.E. Hillard, "Rayleigh scattering measurements in supersonic facilities," AIAA-96-2187, 19th AIAA Advanced Measurement and Ground Testing Technology Conference, New Orleans, LA, June 1996.
21. Tellinghuisen J., The McLennan bands of  $I_2$ : A highly structured continuum. *Chem. Phys. Lett.* 29, pp. 359–363 (1974).
22. Tellinghuisen, J., The ultraviolet laser transitions in  $I_2$  and  $Br_2$ . *Chem. Phys. Lett.* 49, pp. 485–490 (1977).
23. Tellinghuisen, J., Transition strengths in the visible-infrared absorption spectrum of  $I_2$ , *J. Chem. Phys.* 76, pp. 4736–4744 (1982).
24. Tellinghuisen J., The  $D$  ( $O_u^+$ ) state of  $I_2$ : Analysis by quantum simulations of bound-free D-X fluorescence. *Can. J. Phys.* 62, pp. 1933–1940 (1984).
25. Venkateswarlu, P., Vacuum ultraviolet spectrum of the iodine molecule, *Can. J. Phys.* 48, pp. 1055–1080 (1970).

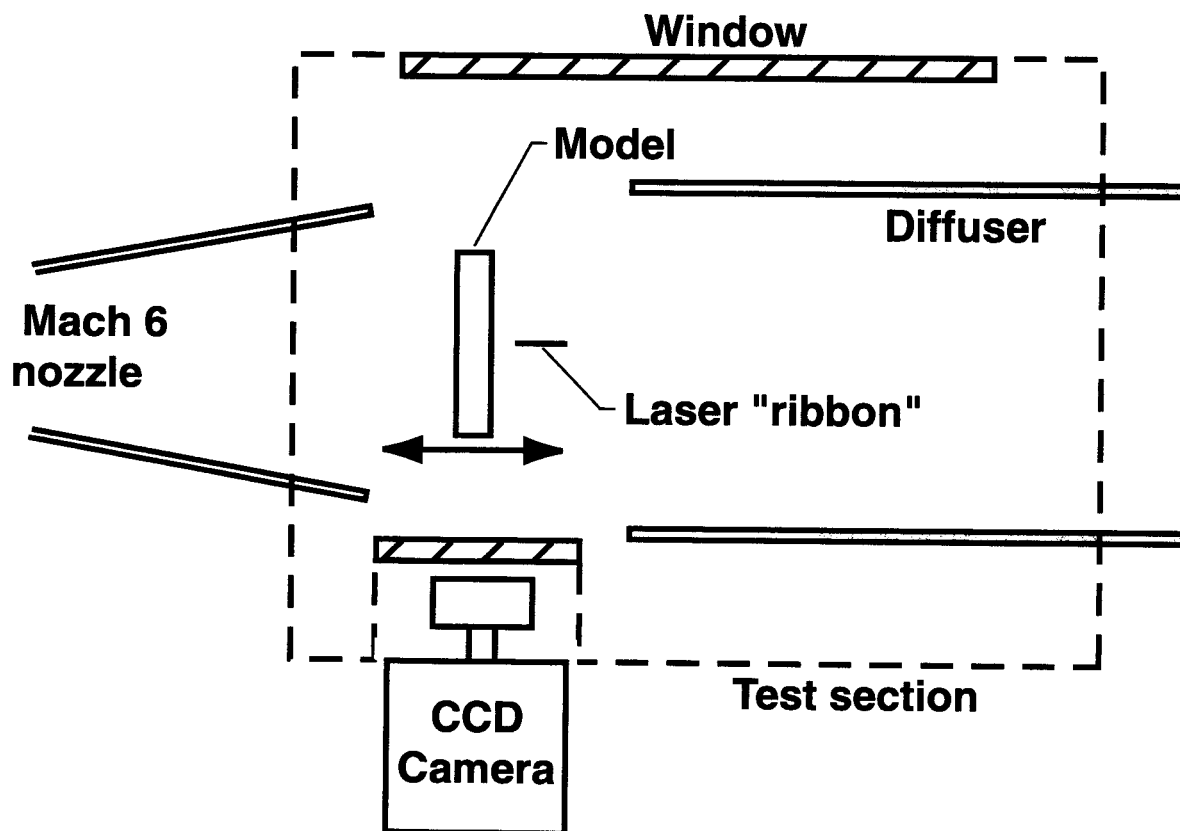


Fig. 1. Simplified schematic diagram of the experimental apparatus.



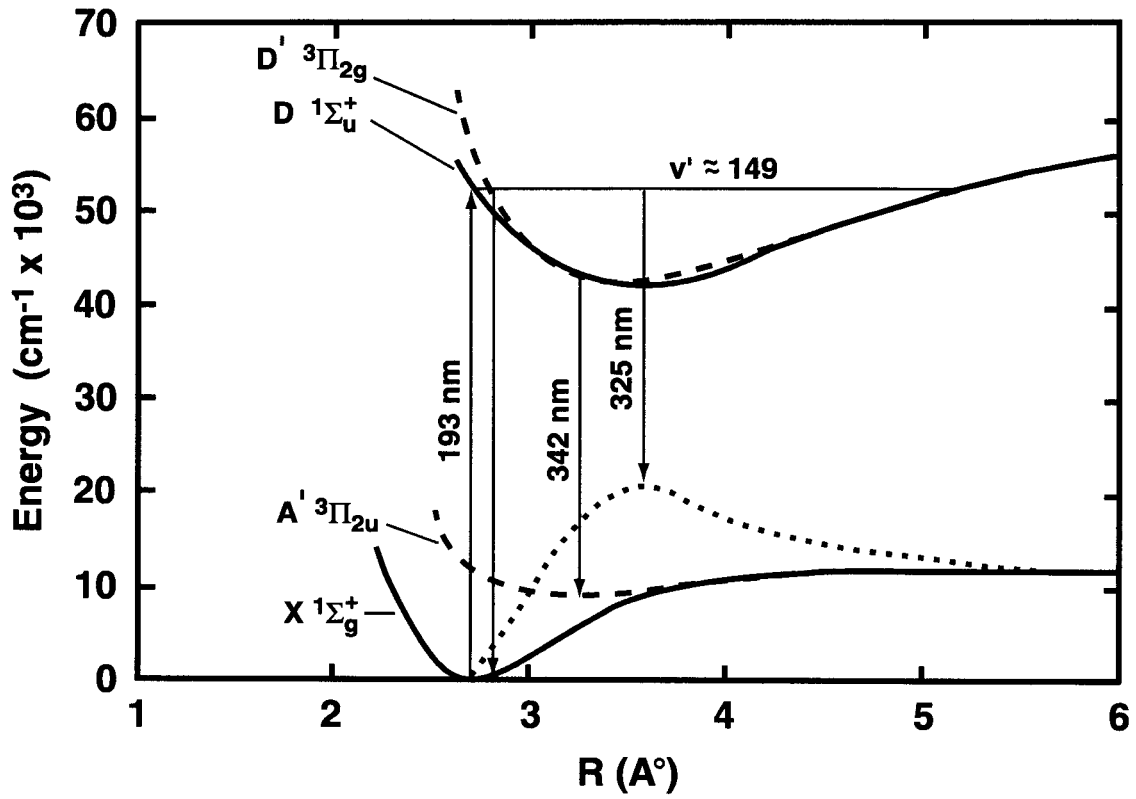


Fig. 2. Simplified I<sub>2</sub> potential curves showing Cordes Band ( $D^1\Sigma_u^+ \leftarrow X^1\Sigma_g^+$ ) absorption using an ArF excimer laser near 193 nm and resulting emission. Bound-bound emission (188–250 nm) and bound-free emission (250–500 nm) occurs from D state. Buffer gas collisions transfer D state population to D' state. This creates 342 nm band emission.

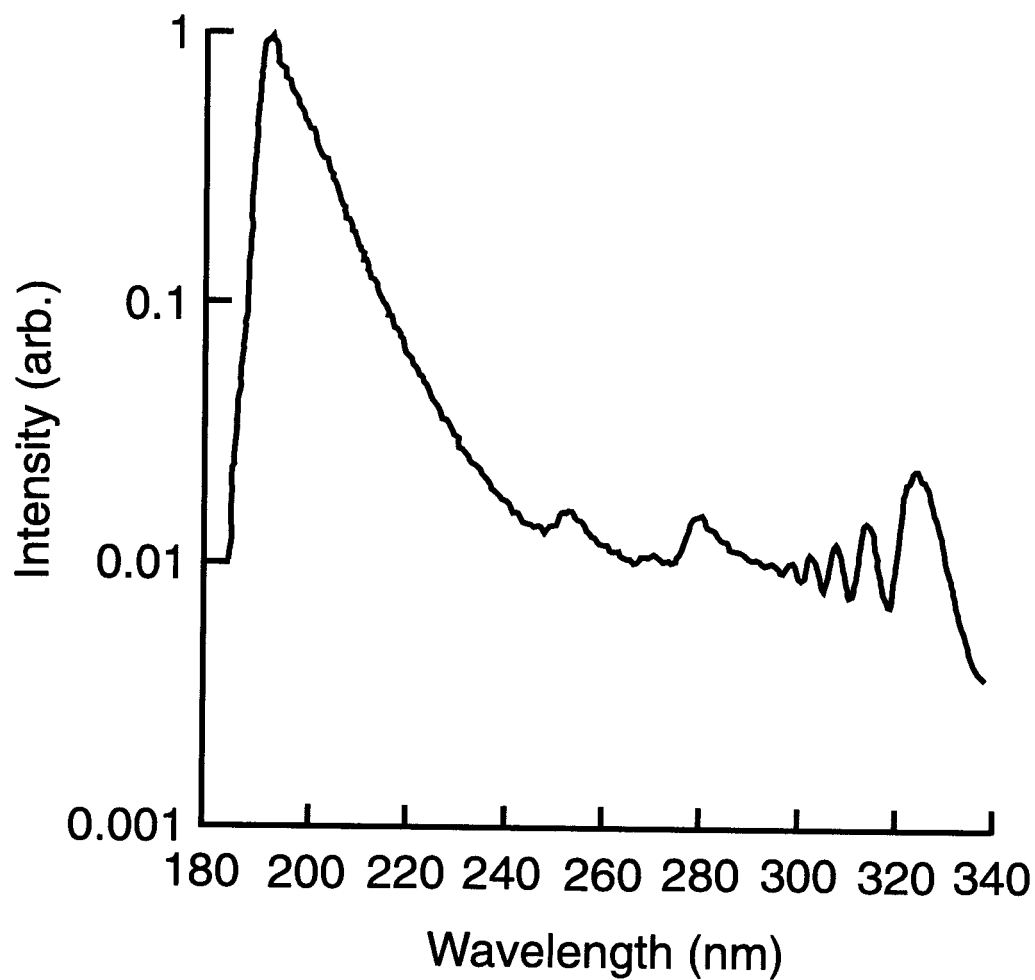


Fig. 3. Low resolution fluorescence emission spectrum of  $7.2 \times 10^{15}$  molecules/cm<sup>3</sup> (0.22 Torr) pure iodine excited using an ArF excimer laser near 193 nm in a 1 cm square Suprasil cell at 295K.

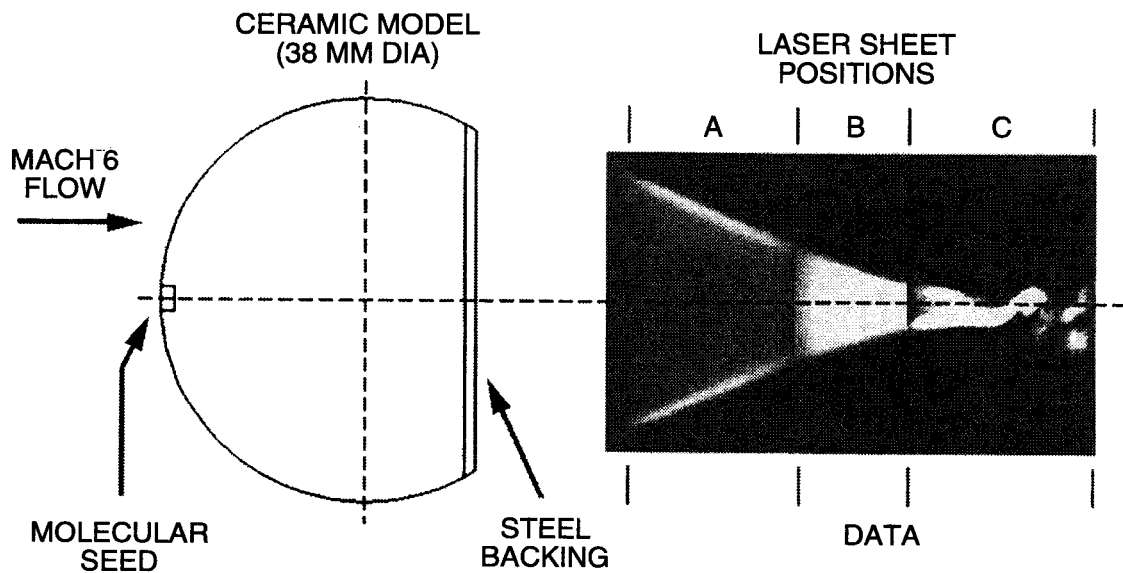


Fig. 4. Composite view to scale of the wake of a truncated cylinder model at Mach 6. The view at laser beam positions A and B are averages of 44 individual frames. A single frame is shown at position C to illustrate the unsteady nature of the flow at this location. Images A and C are 20 mm wide.

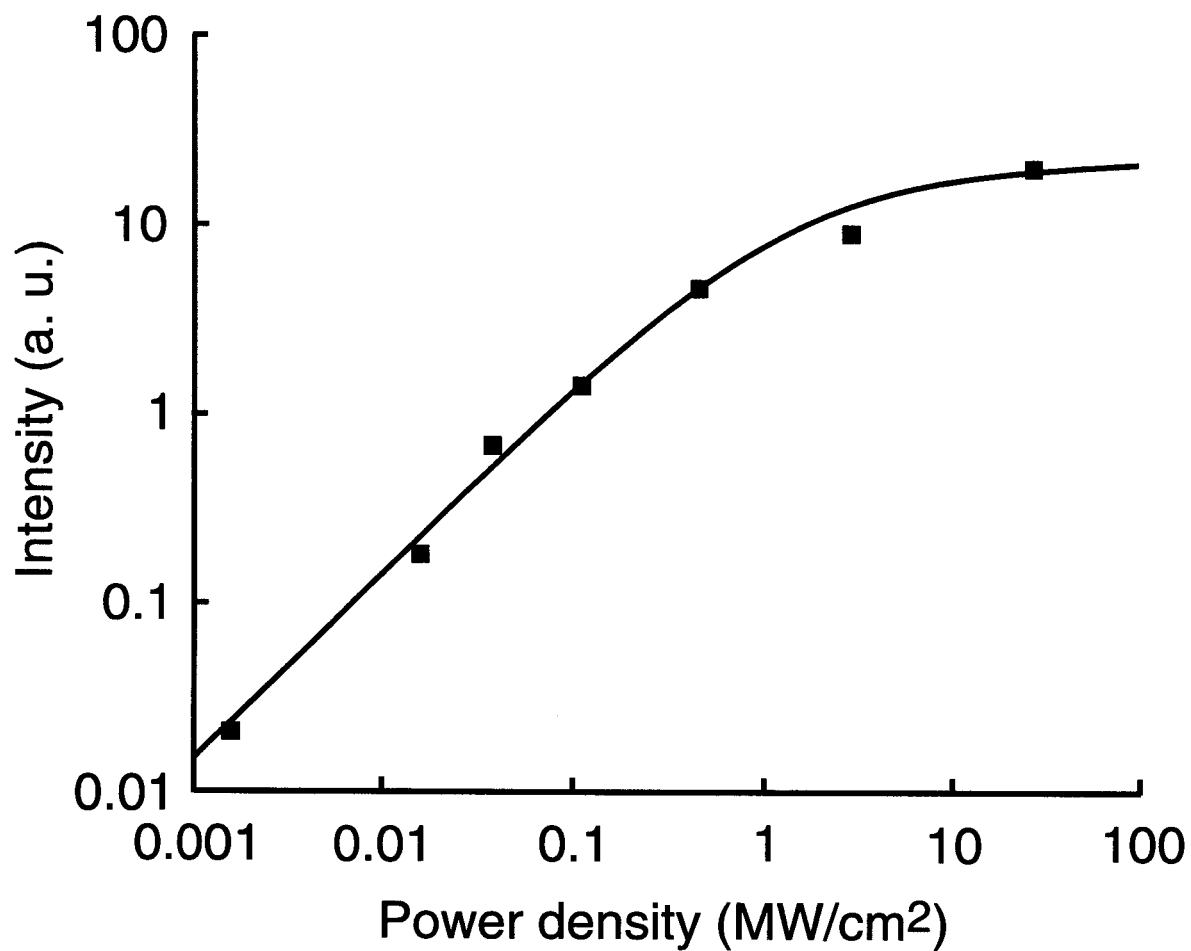


Fig. 5. Optical saturation curve for the bound-bound transitions measured using fluorescence at 325 nm in the McLennan band. Buffer gas is air at a pressure of 1 torr.